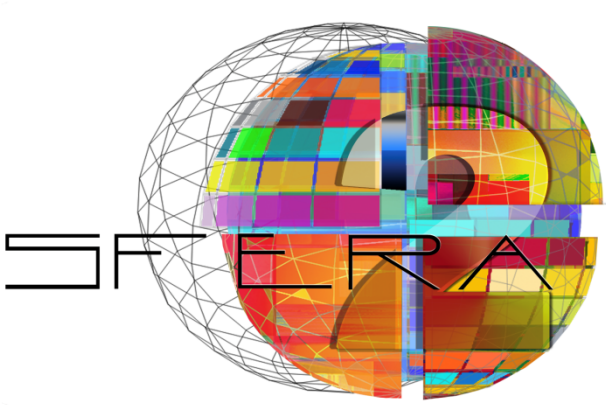

Characterisation of porous materials

Heat and Mass transport properties of reticulated porous ceramic structures

SFERA II Project	
Solar Facilities for the European Research Area -Second Phase	
Grant agreement number:	312643
Start date of project:	01/01/2014
Duration of project:	48 months
WP13 – Task 3.C	Deliverable 13.5
Due date:	03/2015
Submitted	12/2015
File name:	WP13 – Task 3.C Deliverable 13.5
Version	1
Partner responsible	ETHZ
Person responsible	Aldo Steinfeld
Author(s):	Simon Ackermann, Aldo Steinfeld, (Emmanuel Guillot: summary)
Dissemination Level	PU

Executive Summary

The EU-funded research project SFERA2 – grant agreement 312643 – aims to boost scientific collaboration among the leading European research institutions in solar concentrating systems, offering European research and industry access to the best research and test infrastructures and creating a virtual European laboratory.

This deliverable is part of the results of the task 3 of the workpackage 13 *Determination of physical properties of CSP materials under concentrated solar irradiation* within the Joint Research Activities.

This workpackage 13 aims to provide a better evaluation of the material behaviour for CSP applications and other fields with similar thermal stress, such as high temperature steels or SiC ceramics, thanks to better or new experimental tests bed and associated theoretical models. These results will lead to help users developing higher performance materials for higher process efficiency.

The task 3 of workpackage 13 is focused on determining the key properties of porous materials for CSP applications, based on both theoretical and experimental methods:

- Determining heat and mass transfer properties
- Determining physical and chemical surface properties inside the pores

The work presented here focus on the extension of an existing method to predict heat and mass transfer properties with theoretical models from an accurate geometry evaluation by computer tomography.

In this work, a 1D volume-averaged heat and mass transfer model was implemented in a commercial computational fluid dynamics software for characterisation of the heating and reduction performance of complex dual-scale porous ceria structures directly exposed to concentrated solar radiation. The model was based on the numerical resolution of the unsteady mass, momentum, and energy conservation equations by applying the volume-averaging theory for porous media. Additionally, spectroscopic measurements were performed for a high range of wavelengths for the accurate determination of the surface reflectivity of ceria used as validating samples as a function of the reduction extent.

Workpackage 13 overview

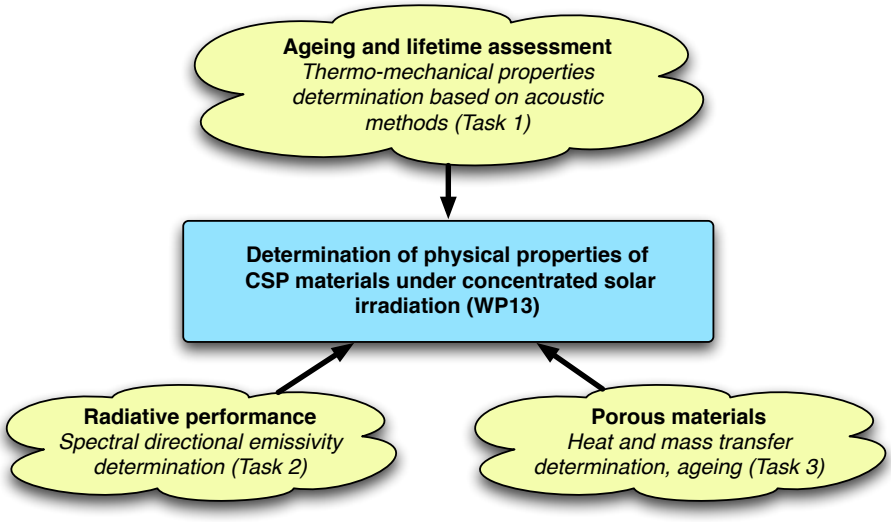

SFERA2 Joint Research Activities : WP13

For completeness, the reader should refer to the other work delivered within the workpackage 13, but also the rest of the project such as WP12 (temperature measurements), WP14 (component qualification) and also the previous project SFERA GA n°228296 such as WP12 task 1 (standardisation activities). http://sfera.sollab.eu/index.php

List of deliverables for SFERA2 WP13:

- Task 1, thermo-mechanical properties
  - D13.1: Selected test samples: materials and geometries selected, modelled behaviour.
  - D13.2: Comparison of the modelled behaviour and experimental results from the developed test bed.
- Task 2, radiative properties
  - D13.3: Comparison of experimental determination of emissivity measurements for selected materials between the techniques used by the partners.
  - D13.4: Assessment of experimental measurements of spectral directional emissivity at high temperature.
- Task 3, porous materials properties
  - ➢ D13.5: Heat and Mass transport properties of reticulated porous ceramic structures.
  - D13.6: Characterisation of the physical and chemical properties of the surface cavities of porous materials.
  - D13.7: Comparison of experimental determination of transport properties to predicted characterisation.

SFERA-II: Report for WP13

7-12-2015

Heat & Mass Transport Properties of Reticulated Porous Ceramic Structures

Authors: S. Ackermann, A. Steinfeld, ETH Zurich

Introduction

Reticulated porous ceramic (RPC) foam-type structures are employed in solar reactors for the thermochemical splitting of H_2O and CO_2 [1]. Optimization of the thermochemical redox cycle demands the development of numerical heat and mass models [2-4]. However, 3D geometrical resolving the porous structures in transient heating and reduction simulations would lead to enormous computational requirements. Thus, the unsteady mass, momentum, and energy conservation equations are numerically solved by applying the volume-averaging theory for porous media [5-9]. In this work, a 1D volume-averaged heat and mass transfer model was implemented in a commercial computational fluid dynamics (CFD) software (ANSYS® Academic Research, release 15.0) for characterisation of the heating and reduction performance of complex dual-scale porous ceria structures directly exposed to concentrated solar radiation. The RPC features dual-scale porosity: mm-size pores for volumetric radiative absorption and effective heat transfer during the reduction step and micron-size interconnected pores within the struts for increased specific surface area leading to enhanced reaction kinetics during the oxidation step [10]. Additionally, spectroscopic measurements were performed for a high range of wavelengths for the accurate determination of the surface reflectivity of ceria as a function of the reduction extent.

Methodology

Porous structures with a high range of porosities and mean pore diameters for the large-scale pores (mm-size) were digitally engineered on the basis of tomography scans of a dual-scale 10 ppi foam with 0.3 strut porosity by either dilation/erosion of the struts with spherical structuring elements on the fluid-solid interface and/or scaling of the actual scan voxel size as schematically shown in Figure 1 [11]. Dilation/erosion of the struts changed slightly the mean pore diameter although the amount of pores per inch stayed constant. The morphology of the dual-scale porous structures were described with the strut porosity, ε_{strut}, the foam porosity ε_{RPC} and the dual-scale porosity ε_{dual} [12]. In this study, the strut morphology was assumed to be constant with a porosity of 0.3 and a mean pore diameter of 10 μm because for this strut morphology a good compromise was shown between a fully connected pore network enhancing the surface limited CO_2 and H_2O splitting rates, high mass loading and stable cycling without destructive sintering of the μm-size pore network [10,12].

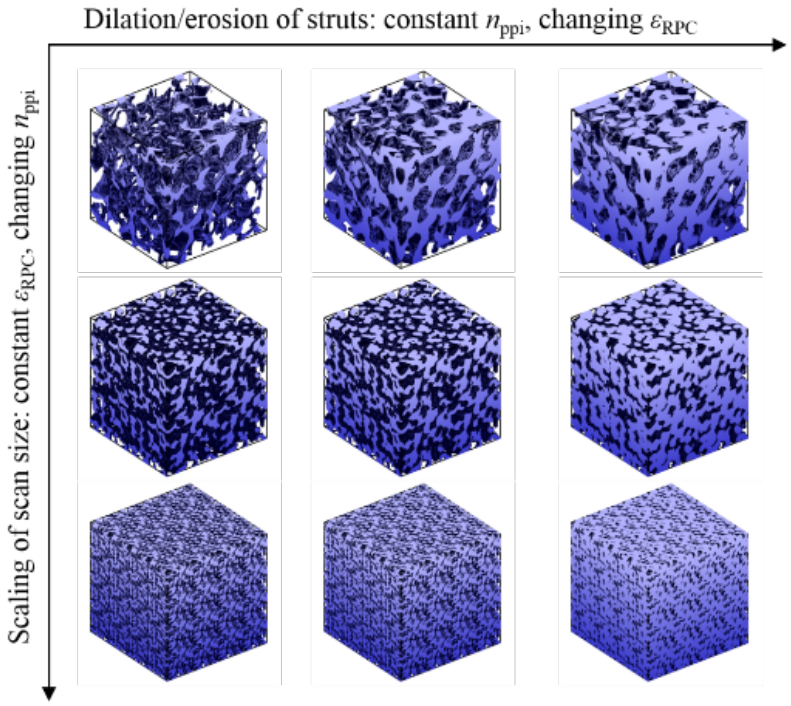

Figure 1: Schematic of 3D structures with a high range of porosities and mean pore diameters for the large-scale pores engineered from the original structure (top-left) obtained with computed tomography

The correlations for describing the morphology and the effective heat and mass transfer within the engineered 3D structures were determined by applying direct pore-level simulations (DPLS) [13-18]. For the determination of the effective conductive heat transfer, the governing Fourier's law within the solid and fluid phase was solved with the finite volume (FV) technique [12,19-23]. For determination of the convective heat transfer coefficient, the permeability and the Dupuit-Forchheimer coefficient, the coupled continuity, momentum and energy (Navier-Stokes) equations were solved with the FV technique [16,24,25]. For the radiative heat transfer characterisation, collision-base Monte Carlo (MC) method was applied to compute the cumulative distribution functions of the attenuation path and the distribution function of the cosine of incidence for extraction of the effective extinction coefficient and the scattering phase function [26].

Thermochemical reduction of a RPC made of ceria

For a cubic porous sample with a volume of 0.025 x 0.025 x 0.025 m^3, ε_{RPC} = 0.75 and $d_{m,RPC}$ = 2.19 mm, Figure 2 shows a) the fluid and solid temperature, b) the intensity of the internal reradiation, c) the nonstoichiometry and d) the oxygen partial pressure as a function of sample depth at different times. Solar radiation enters the structure at z = 0 m and gets volumetrically absorbed. Initially, the near front temperature (z < 0.01 m) increases up to 1500 K in the first 10 s inducing large temperature gradients and stagnates at around 150 s with a maximum temperature of ~2020 K around 0.004 m and < 1300 K at the backside (Figure 2a). Such large steady state temperature gradients are observed because both ends lose 100% of the emitted energy out of the hot domain. The internal reradiation strongly correlates to the solid temperature and peaks at the steady state at around 3.6 W m^{-2} (Figure 2b). The nonstoichiometry reaches values > 0.06 towards the irradiated front while at the backside the structure remains unreduced (Figure 2c). The oxygen partial pressure during the reduction in the structure peaks at to around 0.07 atm at 50 s. Due to the negative feedback of the released oxygen in the purge flow, inducing a change in the oxygen partial pressure, the reduction is still going on even though the temperature reached almost steady state.

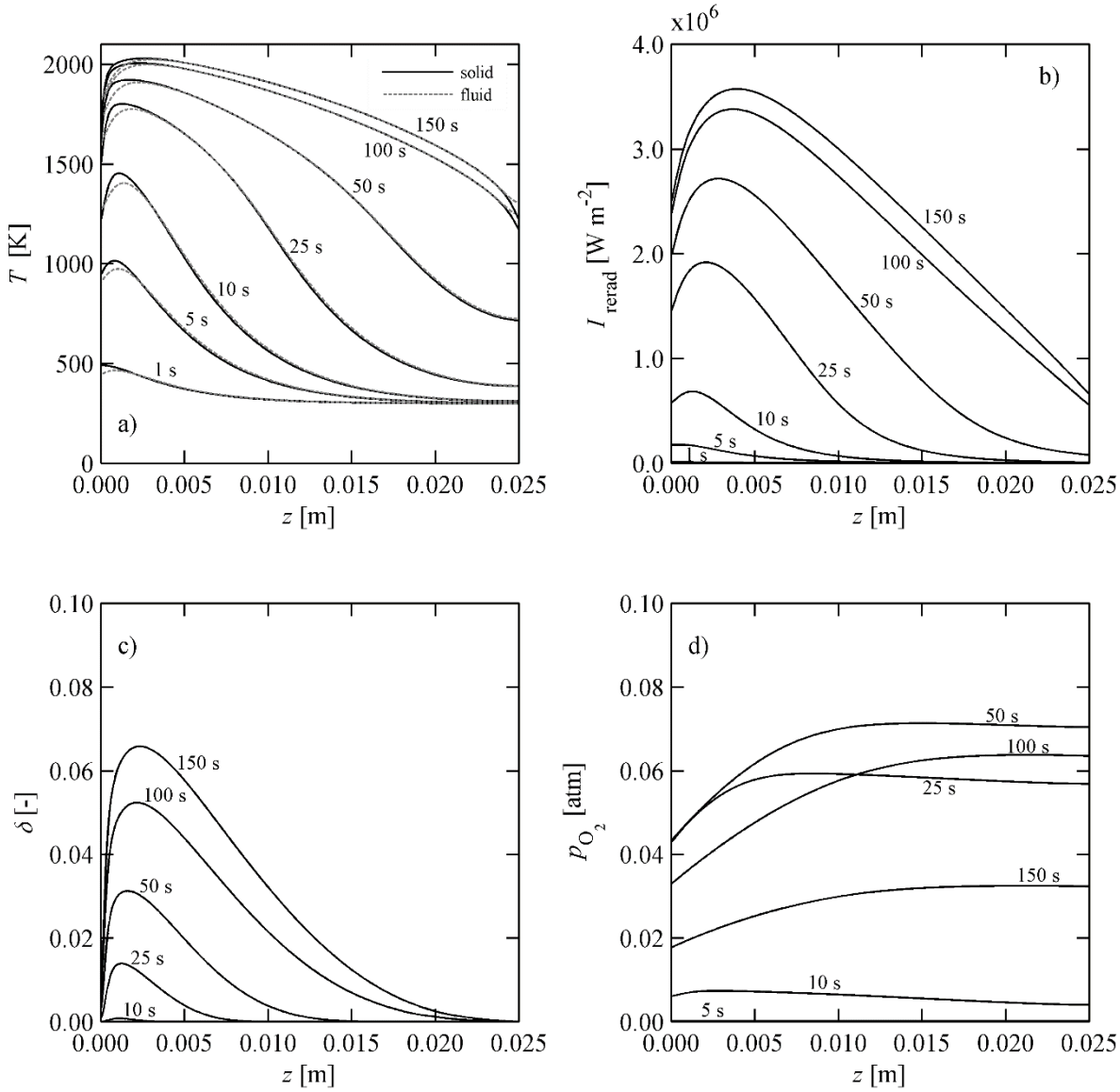

Figure 2: a) Fluid and solid temperature, b) internal reradiation intensity, c) nonstoichiometry, d) oxygen partial pressure in the purge flow through the structure

Experimental validation

Ceria RPC samples with dual-scale porosity were exposed to concentrated radiation at ETH's High-Flux Solar Simulator (HFSS) and reached temperatures above 1873 K under a low oxygen partial pressure. The experimental setup is schematically shown in Figure 3 and consisted of a quartz-glass dome that enables direct irradiation of the RPC samples under controlled gas atmosphere. The ceria RPC samples were then placed into to focus of the HFSS on an inert RPC crucible made of zirconia that allowed a purge flow. The gas composition at the outlet was analysed with a Siemens Ultramat 23 and a gas chromatograph (Varian, CP-4900 Micro GC). The ceria RPC sample was shielded with a 4 mm thick Al_3O_2 insulation. The insulation was surrounded by a water-cooled metallic cooling jacket. Temperature measurements in the ceria RPC were taken at three different depths along radiation penetration: 1: near front region, 2: within the bulk, 3: back side of the RPC. The depth of the thermocouple was around 2-3 mm for the near front region, 8-10 mm for the bulk and 13-14 mm for the back side. Three heating and cooling cycles were performed to ensure reproducibility of the measurement results. The

radiation flux was measured with a calorimeter placed in the focus where the RPC samples were placed and used as the input flux in the simulation.

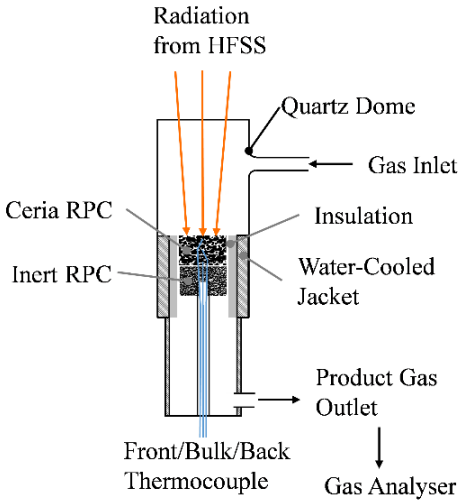

Figure 3: Schematic of the setup for heating of RPC structures with 3 thermocouples at different position along the radiation penetration

The transient results obtained with the simulation were validated in terms of transient temperature and oxygen yield measurements performed with a 10 and 35 ppi ceria RPC. The RPCs were heated in a high flux solar simulator starting from room temperature until the temperature reached steady state as shown in Figure 4a and b. For the near front region, the simulation results agreed well with the temperature measurements and for $t > 50$ s, the model slightly over predicts the temperature measurements. For the bulk and back side, the model initially under predicts the temperature measurements and for the steady state similar temperatures were obtained as shown in Figure 4a. For the simulation and the measurement, the 35 ppi RPC had a higher temperature gradient along the radiation penetration depth compared to the 10 ppi. Additionally, the model agrees well with the transient oxygen yield for both RPC samples as shown in Figure 4b. The nonstoichiometries were calculated by integrating the oxygen concentrations measured with the downstream gas analyser.

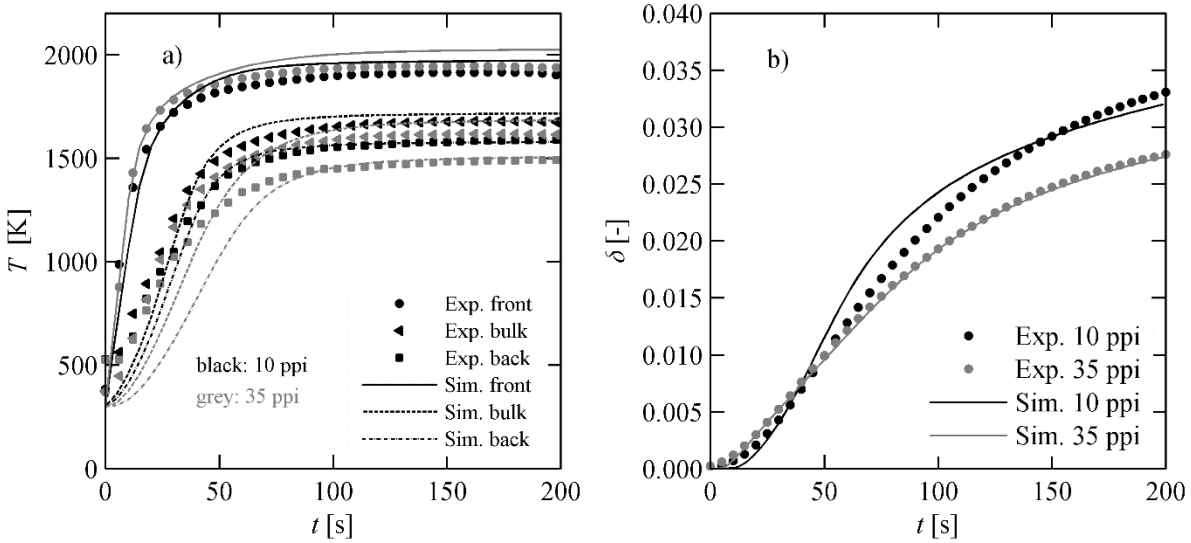

Figure 4: Temporal comparison of simulation results to experimental measurements for a 10 and 35 ppi RPC, a) Temperature at three different depths along to radiation direction, 1: front, 2: in the bulk, 3: back, b) Total nonstoichiometry

References

1. Furler, P.; Scheffe, J.; Gorbar, M.; Moes, L.; Vogt, U.; Steinfeld, A. Solar Thermochemical CO_2 Splitting Utilizing a Reticulated Porous Ceria Redox System. *Energy & Fuels* 2012, *26*, 7051-7059.
2. Furler, P.; Steinfeld, A. Heat Transfer and Fluid Flow Analysis of a 4 kW Solar Thermochemical Reactor for Ceria Redox Cycling. *Chemical Engineering Science* 2015, *137*, 373-383.
3. Keene, D.J.; Davidson, J.H.; Lipiński, W. A Model of Transient Heat and Mass Transfer in a Heterogeneous Medium of Ceria Undergoing Nonstoichiometric Reduction. *Journal of Heat Transfer* 2013, *135*, 052701-052701.
4. Keene, D.J.; Lipiński, W.; Davidson, J.H. The Effects of Morphology on the Thermal Reduction of Nonstoichiometric Ceria. *Chemical Engineering Science* 2014, *111*, 231-243.
5. Bodla, K.K.; Weibel, J.A.; Garimella, S.V. Advances in Fluid and Thermal Transport Property Analysis and Design of Sintered Porous Wick Microstructures. *Journal of Heat Transfer* 2013, *135*, 061202.
6. Kaviany, M. *Principles of Heat Transfer in Porous Media*; 2nd ed.; Springer-Verlag: New York, 1995.
7. Whitaker, S. *The Method of Volume Averaging*; Kluwer Academic: Dordrecht, 1999.
8. Incropera, F.P.; DeWitt, D.P. *Fundamentals of Heat and Mass Transfer*; 5th ed.; J. Wiley: New York, 2002.
9. Bear, J.; Buchlin, J.M. *Modelling and Applications of Transport Phenomena in Porous Media*; Kluwer Academic Publishers: Dordrecht, Netherlands, 1991.
10. Furler, P.; Scheffe, J.; Marxer, D.; Gorbar, M.; Bonk, A.; Vogt, U.; Steinfeld, A. Thermochemical CO_2 Splitting via Redox Cycling of Ceria Reticulated Foam Structures With Dual-Scale Porosities. *Physical Chemistry Chemical Physics* 2014, *16*, 10503-10511.
11. Suter, S.; Steinfeld, A.; Haussener, S. Pore-Level Engineering of Macroporous Media for Increased Performance of Solar-Driven Thermochemical Fuel Processing. *International Journal of Heat and Mass Transfer* 2014, *78*, 688-698.
12. Ackermann, S.; Scheffe, J.R.; Duss, J.; Steinfeld, A. Morphological Characterization and Effective Thermal Conductivity of Dual-Scale Reticulated Porous Structures. *Materials* 2014, *7*, 7173-7195.
13. Haussener, S.; Steinfeld, A. Effective Heat and Mass Transport Properties of Anisotropic Porous Ceria for Solar Thermochemical Fuel Generation. *Materials* 2012, *5*, 192-209.
14. Bodla, K.K.; Murthy, J.Y.; Garimella, S.V. Microtomography-Based Simulation of Transport through Open-Cell Metal Foams. *Numerical Heat Transfer Part A-applications* 2010, *58*, 527-544.
15. Krishnan, S.; Murthy, J.Y.; Garimella, S.V. Direct Simulation of Transport in Open-Cell Metal Foam. *Journal of Heat Transfer* 2006, *128*, 793-799.
16. Haussener, S.; Jerjen, I.; Wyss, P.; Steinfeld, A. Tomography-Based Determination of Effective Transport Properties for Reacting Porous Media. *ASME Conference Proceedings* 2010, *2010*, 883-892.
17. Haussener, S.; Coray, P.; Lipinski, W.; Wyss, P.; Steinfeld, A. Tomography-Based Heat and Mass Transfer Characterization of Reticulate Porous Ceramics for High-Temperature Processing. *Journal of Heat Transfer* 2010, *132*, 023305-1.
18. Friess, H.; Haussener, S.; Steinfeld, A.; Petrasch, J. Tetrahedral Mesh Generation Based on Space Indicator Functions. *International Journal for Numerical Methods in Engineering* 2013, *93*, 1040-1056.
19. Petrasch, J.; Schrader, B.; Wyss, P.; Steinfeld, A. Tomography-Based Determination of the Effective Thermal Conductivity of Fluid-Saturated Reticulate Porous Ceramics. *ASME Journal of Heat Transfer* 2008, *130*, 032602-1.
20. Petrasch, J.; Wyss, P.; Stämpfli, R.; Steinfeld, A. Tomography-Based Multiscale Analyses of the 3D Geometrical Morphology of Reticulated Porous Ceramics. *Journal of the American Ceramic Society* 2008, *91*, 2659-2665.
21. Coquard, R.; Loretz, M.; Baillis, D. Conductive Heat Transfer in Metallic/Ceramic Open-Cell Foams. *Advanced Engineering Materials* 2008, *10*, 323-337.
22. Boomsma, K.; Poulikakos, D. On the Effective Thermal Conductivity of a Three-Dimensionally Structured Fluid-Saturated Metal Foam. *International Journal of Heat and Mass Transfer* 2001, *44*, 827-836.
23. Bhattacharya, A.; Calmidi, V.V.; Mahajan, R.L. An Analytical-Experimental Study for the Determination of the Effective Thermal Conductivity of High Porosity Fibrous Foams. *ASME Applied Mechanics Division-Puplication-AMD* 1999, *233*, 13-20.
24. Petrasch, J.; Meier, F.; Friess, H.; Steinfeld, A. Tomography Based Determination of Permeability, Dupuit-Forchheimer Coefficient, and Interfacial Heat Transfer Coefficient in Reticulate Porous Ceramics. 2008, *29*, 12.
25. Zermatten, E.; Haussener, S.; Schneebeli, M.; Steinfeld, A. Tomography-based determination of permeability and DupuitForchheimer coefficient of characteristic snow samples. *Journal of Glaciology* 2011, *57*, 811-816.
26. Petrasch, J.; Wyss, P.; Steinfeld, A. Tomography-Based Monte Carlo Determination of Radiative Properties of Reticulate Porous Ceramics. *Journal of Quantitative Spectroscopy and Radiative Transfer* 2007, *105*, 180-197.